

Towards Accurate Crop Yield Prediction: Integrating Sentinel-2 Remote Sensing with AI-Based Modelling

Esmail Abdali, Emadoddin Hemmati, Niloofar Alizadeh, Hamed Amini Amirkolae *

Basysco Remote Sensing Institute, Tehran, Iran - esmailabdalli@basysco.com, aradhemmati@basysco.com,
niloofar.alizadeh@basysco.com, hamed.amini@basysco.com

Commission IV, WG IV/3

KEY WORDS: Artificial Intelligence, Canopy, Leaf Area Index, Remote Sensing, Sentinel-2.

ABSTRACT:

Accurate monitoring of vegetation health and canopy structure is essential for optimizing agricultural productivity and managing natural resources. Remote sensing technologies, combined with artificial intelligence (AI) and advanced satellite data, have revolutionized the capacity to assess crop conditions at large scales with high temporal and spatial resolution. This study leverages Sentinel-2 multispectral imagery and a novel AI-driven model approach to estimate Leaf Area Index (LAI) across multiple fields for canola. By integrating spectral reflectance data with view and solar geometry parameters, the model effectively captures the complex interactions between canopy structure and environmental factors. The methodology employs a two-layer neural network calibrated with physically based normalization to translate Sentinel-2 spectral and angular inputs into accurate LAI estimates. Validation against observed field measurements demonstrates strong agreement, underscoring the model's robustness and reliability. Spatial analysis reveals distinct LAI patterns among the crop types, highlighting differences in canopy density and growth dynamics. Temporal profiling further illustrates crop-specific development trends, with canola showing extended canopy expansion. The results confirm that the fusion of remote sensing data with AI modelling provides a powerful tool for precision agriculture, enabling detailed monitoring of crop growth and facilitating informed decision-making. This approach offers significant potential for enhancing yield prediction, resource management, and sustainable farming practices, ultimately supporting global food security efforts.

1. INTRODUCTION

Agriculture is a fundamental sector that sustains human life by providing food, fibre, and raw materials (Weiss et al., 2022; Sishodia et al., 2020). In modern agriculture, effective monitoring and management of crop production are essential to meet the increasing global demand for food, reduce environmental impacts, and enhance sustainability (Padilla et al., 2020). Crop monitoring is a vital process involving continuous observation and precise assessment of the various factors that influence agricultural productivity (Csikós et al., 2023). These factors include soil conditions, water resources, plant health, and climatic variables such as solar radiation, temperature, humidity, and wind. Comprehensive monitoring enables farmers and agricultural experts to make informed decisions aimed at improving yield, optimizing input use, and minimizing environmental degradation (Srivastav et al., 2021; Romero et al., 2024; Zhao et al., 2024; Kirk et al., 2025).

Remote sensing technology has emerged as a powerful tool in agricultural monitoring. Satellite imagery, drone-based sensors, and ground-based devices collect valuable spatial and temporal data on crop and soil conditions at local to regional scales (Hemmati et al., 2024; Abdali et al., 2024). Among satellite platforms, Sentinel-2, with its high spatial resolution multispectral imagery, has gained widespread attention for agricultural applications (Segarra et al., 2020). It provides timely, multi-temporal data that allows accurate mapping of vegetation indices, soil moisture, crop health, and phenological stages (Hassanpour et al., 2024; Pokhariyal et al., 2023). When combined with advanced data processing techniques, such as artificial intelligence (AI) and machine learning (ML), remote

sensing data can be transformed into actionable insights. AI algorithms can analyse complex patterns in large datasets, identify disease outbreaks, detect nutrient deficiencies, and forecast crop yields with improved accuracy (Alshaya et al., 2025; Wang et al., 2024). This integration of remote sensing and AI supports precision agriculture practices that lead to enhanced resource efficiency, reduced costs, and improved crop quality, ultimately contributing to sustainable agricultural systems (Wang et al., 2025).

The use of remote sensing for agricultural land management is a well-established research domain driven by the urgent need to increase food production sustainably amid rising global populations. Remote sensing provides real-time, large-scale, and cost-effective data on soil properties, vegetation cover, water availability, and climate conditions (Mostafiz et al., 2021; L et al., 2024). This enables continuous and detailed monitoring of crop status with minimal human intervention. The advent of high-resolution satellites such as Landsat, MODIS, and Sentinel-2 has accelerated the adoption of remote sensing in agriculture by offering rich spectral and spatial information. Vegetation indices like NDVI (Normalized Difference Vegetation Index) derived from these datasets serve as key indicators of plant biomass, vigour, and stress factors.

Recent advances in ML and AI have significantly enhanced the utility of remote sensing data in agriculture. These technologies excel at processing vast volumes of satellite data to uncover complex relationships among environmental variables and crop performance. For example, deep learning models have been successfully applied to detect plant diseases, identify pest infestations, and predict crop yields. These AI-driven approaches outperform traditional statistical methods by

* Corresponding author

capturing nonlinear patterns and interactions in heterogeneous agricultural landscapes (Hemmati et al., 2024).

Several studies have demonstrated the potential of Sentinel-2 imagery for precision agriculture. Escolà et al. (2017) evaluated Sentinel-2A data for barley crop monitoring, using multiple vegetation indices to correlate with yield data collected from combine harvesters (Escolà et al., 2021). Although vegetation indices based on green reflectance showed moderate correlation (highest R^2 around 0.48), results indicated that earlier imagery and additional indices could improve accuracy. Bukowiecki et al. (2021) combined Sentinel-2 data with UAV-derived Green Area Index (GAI) for winter wheat monitoring, achieving a high predictive performance ($R^2 = 0.82$) in estimating GAI and correlating it with final grain yield. However, they noted Sentinel-2's limitations in capturing spatial variability due to its spectral and temporal resolution constraints.

Segarra (2024) detailed the application of satellite imagery—including Landsat 9, Sentinel-2, and commercial satellites—in precision agriculture, emphasizing data management, processing challenges, and the role of cloud computing (Segarra et al., 2020). Nguyen et al. (2022) used time-series Sentinel-2 images to map canola yield in Alberta, applying random forest and linear regression models (Nguyen et al., 2022). They achieved yield prediction accuracies within 12-16% error margins, demonstrating that moderate-resolution satellite data can detect small-scale yield variations. Zhao et al. (2023) deployed deep learning (U-Net architecture) for precise lavender field segmentation using Sentinel-2 spectral bands, attaining a Dice coefficient of 0.8324, highlighting the effectiveness of AI in crop classification (Zhao et al., 2023).

A comprehensive review by Wang et al. (2024) analysed the integration of remote sensing and machine learning in precision agriculture over the past decade (Wang et al., 2024). They found hyperspectral remote sensing and UAV data to be highly promising, with support vector machines and random forests as leading algorithms. Challenges such as data acquisition, model interpretability, and generalizability remain, alongside trends toward increased automation and international collaboration.

While satellite data offers a broad perspective for crop monitoring and yield estimation, limitations persist in heterogeneous small-scale farming systems due to spatial resolution and cloud cover issues.

Our work presents an innovative yield estimation approach by integrating Sentinel-2 satellite imagery with the WOFOST¹ crop growth simulation model, combining real-time remote sensing data with process-based crop physiology. This hybrid method dynamically calibrates WOFOST parameters using Sentinel-2's spatially detailed information on vegetation status, enabling more accurate crop growth and yield predictions by overcoming limitations of using either satellite data or models alone. The integration supports continuous monitoring over large areas, improving decision-making for precision agriculture practices like fertilization and irrigation, while also aiding risk assessment through scenario simulations. By addressing challenges such as Sentinel-2's spectral and temporal constraints, our system enhances yield estimate reliability and incorporates climatic and soil variables not easily captured by satellite imagery alone.

¹ World Food Studies

2. MATERIAL AND METHOD

2.1 Case study

The study area is located within the geographic coordinates ranging approximately from 31.960°N to 31.980°N latitude and from 48.600°E to 48.640°E longitude. This region encompasses a diverse agricultural landscape characterized by fields of canola, as verified by ground truthing (Figure 1). The agricultural parcels are distributed along a riverine environment, with irrigated fields primarily situated near the water source. The spatial extent covers roughly a 2 km by 0.02° latitudinal strip within these coordinate bounds, featuring a mix of crop types and varying field sizes.

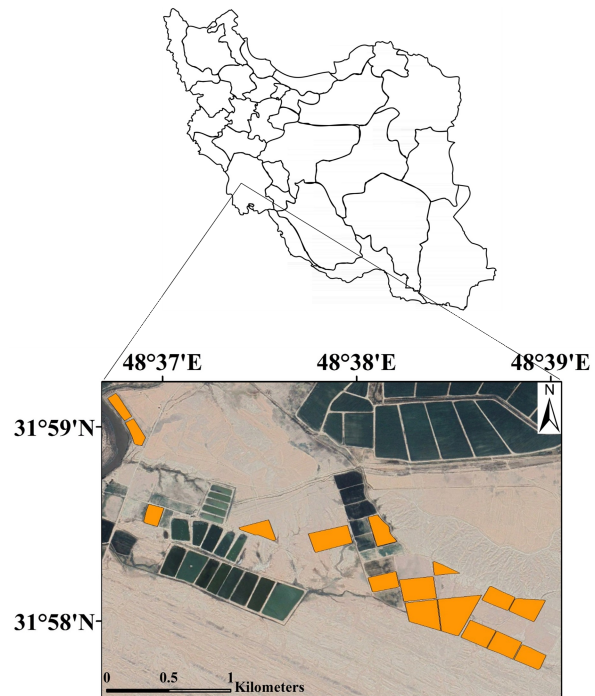


Figure 1. Study area.

2.2 Dataset

2.2.1 Ground Truth Dataset

For validation, we obtained field boundary shapefiles of one crop type, canola, from Mian Bandan Cultivation and Industry Company, a leading agribusiness in the study region. These shapefiles provide precise georeferenced polygons of cultivated fields, enabling accurate alignment with Sentinel-2 data. Field-specific attributes, including harvested yields, sowing dates, irrigation dates and amounts, as well as fertilizer application dates and quantities, were recorded during site visits. This ensured reliable ground truth data for model training and validation.

2.2.2 Satellite Dataset

Sentinel-2 is a powerful Earth observation satellite with 13 spectral bands at varying resolutions 10m, 20m, and 60m, making it ideal for precision agriculture (Abdali et al., 2024). The 10-meter bands which are visible and near-infrared—B2, B3, B4, B8 provide detailed crop health and land cover mapping, while the 20-meter bands which are red edge and shortwave infrared—B5, B6, B7, B11, B12 help detect plant stress, water content, and soil conditions. The 60-meter bands

(B1, B9, B10) are used for atmospheric correction and haze detection. With a 5-day revisit time, Sentinel-2 delivers frequent, high-quality imagery for monitoring crop growth, optimizing irrigation, and improving yield predictions, supporting data-driven farming decisions (Nguyen et al., 2021; Li et al., 2022).

2.3 Methodology

2.3.1 Estimation of Leaf Area Index from Sentinel-2 Data

The Leaf Area Index (LAI) is estimated using a physically informed approach that integrates Sentinel-2 multispectral reflectance data (green, red, and near-infrared bands) with sensor and solar geometry parameters (Liu et al., 2024). The method employs a two-layer neural network to process normalized spectral reflectance and angular data (sun and view angles), which are adjusted to enhance model sensitivity to canopy structure. Sentinel-2 imagery is pre-processed through spatial cropping and spectral normalization to minimize atmospheric and sensor-related inconsistencies (Djamai et al., 2019). The neural network outputs denormalized LAI values, enabling high-resolution, pixel-level estimation of vegetation canopy density across diverse agricultural landscapes. This approach ensures robustness under varying seasonal and environmental conditions, making it suitable for precision agriculture applications. For each of the 12 study fields, LAI values are averaged across all valid pixels to produce a single representative LAI per field. This step accounts for intra-field heterogeneity while maintaining the spatial resolution relevant to agronomic decision-making.

The Leaf Area Index (LAI) is computed through a two-layer neural network model processing normalized spectral and angular data:

First, spectral bands and angular parameters are normalized to $[0,1]$ range as shown in equation (1-6):

$$Green_{norm} = Green - 00.2434 \quad (1)$$

$$Red_{norm} = Red - 00.2951 \quad (2)$$

$$NIR_{norm} = \frac{NIR - 0.0213}{0.7538 - 0.0213} \quad (3)$$

$$\theta_v^{norm} = \frac{\cos(\theta_v) - 0.9796}{0.9999 - 0.9796} \quad (4)$$

$$\theta_s^{norm} = \frac{\cos(\theta_s) - 0.3421}{0.9275 - 0.3421} \quad (5)$$

$$\phi^{norm} = \frac{\cos(\phi_s - \phi_v) - (-1)}{1 - (-1)} \quad (6)$$

where: θ_v, ϕ_v : View zenith and azimuth angles
 θ_s, ϕ_s : Solar zenith and azimuth angles
 $\phi = \phi_s - \phi_v$: Relative azimuth angle

For each neuron i (1 to 5) hidden layer computation is shown in Equation 7-10:

$$n_i = b_i^{(1)} + \sum_{j=1}^5 w_{ij}^{(1)} \cdot x_j \quad (7)$$

Where input vector:

$$x = [Green_{norm}, Red_{norm}, NIR_{norm}, \theta_v^{norm}, \theta_s^{norm}, \phi^{norm}] \quad (8)$$

$$[b_i^{norm}, \phi^{norm}]$$

Bias vector:

$$b^{(1)} = [-2.9498, 1.2221, 1.3544, -1.4519, 2.7030] \quad (9)$$

Weight matrix:

$$W^{(1)} = \begin{bmatrix} 1.3180 & \dots & -0.8921 \\ \vdots & \ddots & \vdots \\ 1.7114 & \dots & -1.9757 \end{bmatrix} \quad (10)$$

Hyperbolic tangent sigmoid (tanh) applied to each n_i to compute activation function in Equation (11):

$$tansig(n_i) = \frac{2}{1 + e^{-2n_i}} - 1 \quad (11)$$

The output layer is:

$$LAI_{norm} = b^{(2)} + \sum_{i=1}^5 w_i^{(2)} \cdot tansig(n_i) \quad (12)$$

Parameters:

$$b^{(2)} = 0.3667$$

$$w^{(2)} = [0.0017, -0.0071, -0.4429, 0.9504, 0.0092] \quad (13)$$

Then applies denormalization:

$$LAI = LAI_{norm} \times 13.8346 + 0.0002 \quad (14)$$

Finally, a Spatial Aggregation is applied for each field k as could be seen in Equation (15):

$$LAI_k = \frac{1}{N_k} \sum_{p=1}^{N_k} LAI_p \quad (15)$$

Where N_k is the number of valid pixels within the field boundary.

2.3.2 Estimation of Ideal Crop Growth Parameters

The ideal crop growth scenario is derived by analysing historical and current LAI data from the WOFOST (World Food Studies) crop growth model. By comparing WOFOST-simulated LAI values from previous and current growing seasons, we calculate the area under the curve (AUC) to determine the ratio of optimal growth conditions. This ratio represents the theoretical maximum LAI achievable under ideal agronomic management, excluding stressors such as water deficits, nutrient limitations, or pest damage. The derived ideal LAI serves as a benchmark for assessing potential crop performance in the study area.

2.3.3 Potential Crop Yield Estimation

Potential crop yield is estimated by scaling the ideal growth parameters (Section 2.3.2) to field-observed conditions. The ratio between the ideal LAI (from WOFOST) and the actual LAI (estimated via Sentinel-2) is applied to adjust theoretical yield projections. This adjustment accounts for suboptimal growth conditions, such as variations in soil fertility, water availability, or management practices. The final yield estimate is computed by integrating this ratio with field-specific agronomic data, providing a spatially explicit prediction of harvestable yield under real-world constraints.

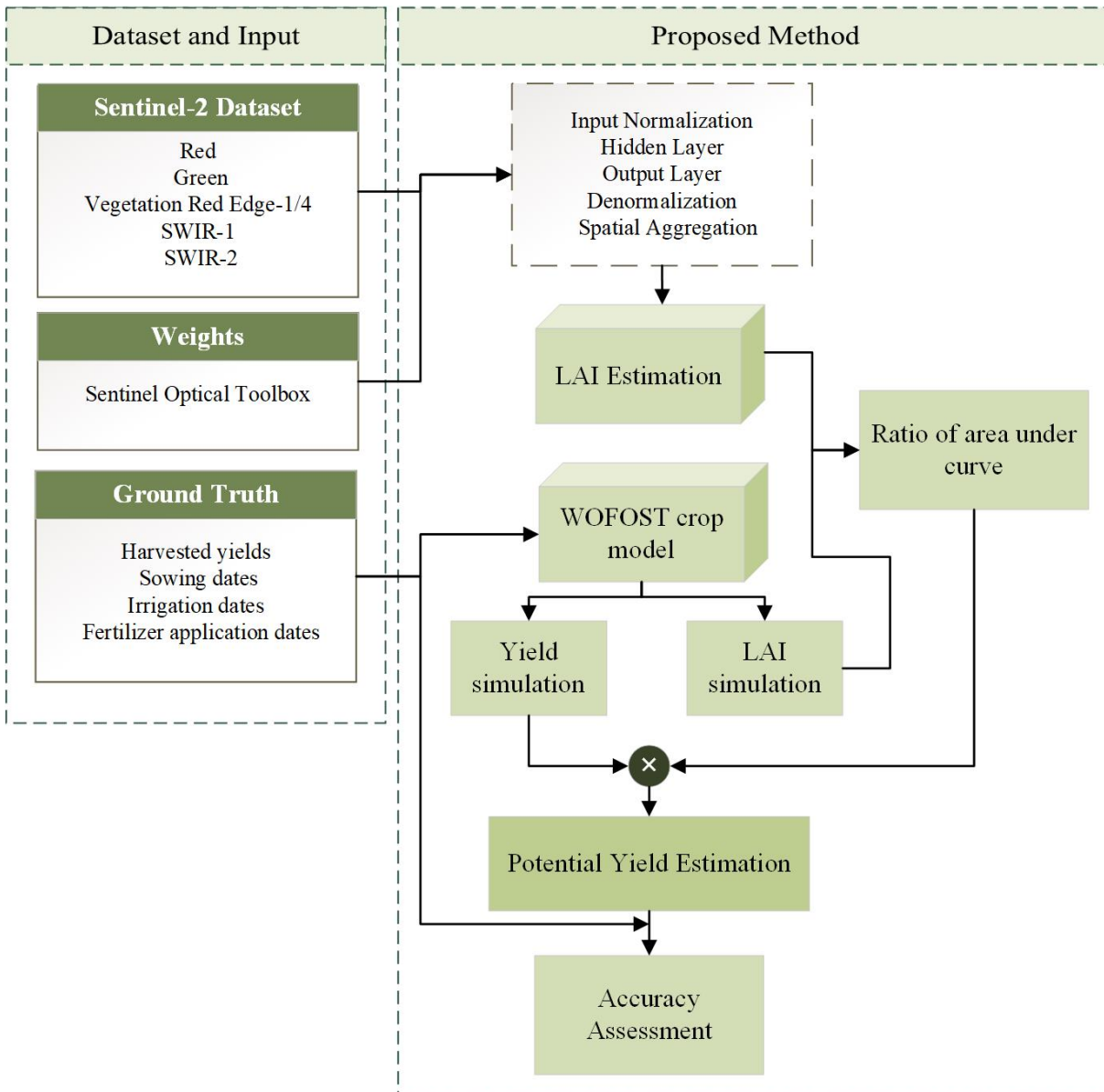


Figure 2. Workflow of this study.

3. RESULT

The results presented here demonstrate the effectiveness of the proposed LAI estimation method across multiple crop types and growing seasons. By integrating Sentinel-2 satellite data with a physically based modelling approach, the study successfully captured spatial and temporal variations in canopy development. Validation against observed field measurements confirmed the model’s accuracy and robustness, highlighting its potential for precise monitoring of crop growth dynamics. The following sections detail the analysis of LAI patterns across different crops, the agreement between observed and simulated values, and the temporal trends in canopy development throughout the growing season.

3.1 LAI Analysis Across Different Fields

This study conducted a comprehensive analysis of LAI dynamics across three key fields of Canola. LAI values were assessed using both observed field measurements and model simulations over current and previous growing seasons to capture temporal and inter-annual variability. The results revealed distinct canopy development patterns among the fields. Field 1, Figure 3a, exhibited an LAI range of approximately 0 to 3.5, with canopy development peaking around mid-season (100–150 days). Field 2, Figure 3b, showed a similar LAI range but with an extended growth duration, up to 250 days, suggesting prolonged canopy density. Field 3, Figure 3b, mirrored the LAI range of the other fields, 0 to 3.5, but achieved higher mid-season values (-1.5), indicating rapid early-stage canopy expansion.

These variations underscore the influence of field-specific conditions, such as planting dates and management practices, on

Canola's phenological progression and canopy architecture. The integrated modelling approach successfully quantified these differences, demonstrating its utility for precision agriculture applications.

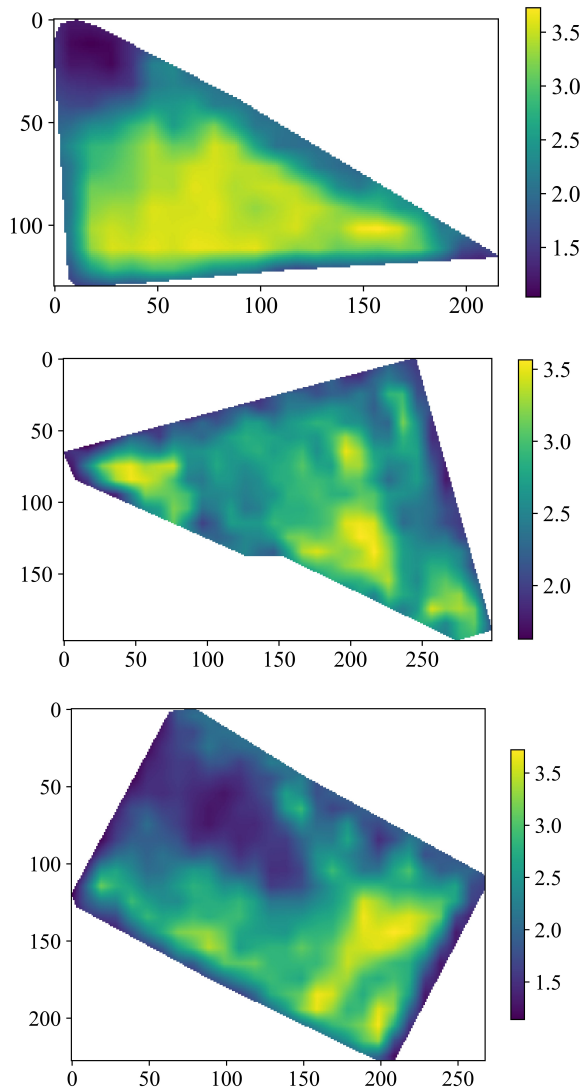


Figure 3. Spatial distribution of simulated LAI for Canola. (a), Field 1 (b) Field 2, and (c) Field 3.

3.2 Observed vs. Simulated LAI Validation

The scatter plot analysis validates the LAI estimation method by comparing model-predicted values against field-observed LAI measurements across the three Canola fields which its values are represented in Figure 4. The plot displays reported (observed) LAI values on the x-axis and estimated (modelled) LAI values on the y-axis, with reference lines including the 1:1 line ($y = x$) and several horizontal thresholds ($y = 400, 1400, 1600, 1800, 2000$) to assess estimation accuracy across different LAI ranges.

The model's performance is quantified by an $RMSE^2$ of 208.81 and an R^2 of 0.70, indicating a strong correlation between predicted and observed LAI values. Most data points cluster

² Root Mean Square Error

near the 1:1 line, demonstrating that the physically informed neural network approach, which integrates Sentinel-2 reflectance data and angular geometry, effectively captures canopy density variations in Canola. Minor deviations occur at higher LAI values (1600–2600), likely due to field-specific factors such as canopy closure or sensor saturation.

The scatter plot further highlights the method's robustness in addressing intra-field heterogeneity. By averaging LAI estimates across all valid pixels per field, the model accounts for spatial variability while aligning with agronomic decision-making scales. The integration of WOFOST-derived ideal LAI benchmarks (Section 2.3.2) contextualizes discrepancies, revealing where suboptimal conditions (e.g., water stress) may have reduced actual LAI relative to potential. This validation confirms the utility of the combined remote sensing and process-based modelling approach for precision agriculture in Canola systems.

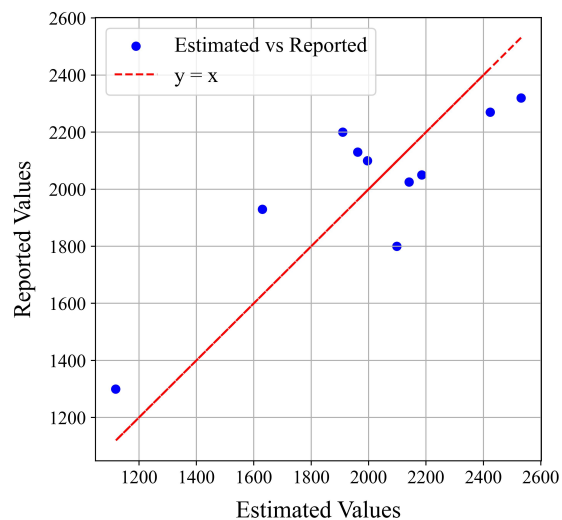


Figure 4. Scatter plot comparing observed versus simulated LAI values for Canola.

3.3 Time-Series Analysis of Canola LAI Dynamics

The time-series analysis of LAI provided detailed insights into the temporal dynamics of canopy development for canola across three distinct fields (Figure 5). The observed data revealed that canola exhibited a prolonged canopy expansion phase, with LAI values increasing steadily before reaching peak canopy density later in the growing season. This extended growth period aligns with canola's physiological traits, which favour gradual but sustained leaf area development.

The model simulations for both current and previous growing seasons closely tracked the observed LAI trends across all three fields, demonstrating strong agreement in capturing seasonal growth patterns. Field 2 (Figure 5b) displayed a slightly earlier peak in LAI, suggesting favourable early-season conditions. Field 1 (Figure 5a) showed a more gradual increase with sustained high LAI values, indicative of optimal mid-to-late season growth. Field 3 (Figure 5c) exhibited some interannual variability, with the current year's simulation aligning more closely with observations than the prior year's, possibly due to improved model calibration or differing weather conditions.

The model's ability to accurately replicate these temporal trends underscores its utility for precision agriculture applications. Specifically, it enables optimization of input management such as irrigation and fertilization by identifying critical growth

phases, supports yield forecasting through continuous monitoring of canopy health, and facilitates risk assessment by comparing current growth against historical baselines. This analysis confirms that the integrated modelling framework effectively captures canola's unique phenology, providing a reliable tool for field-specific decision-making.

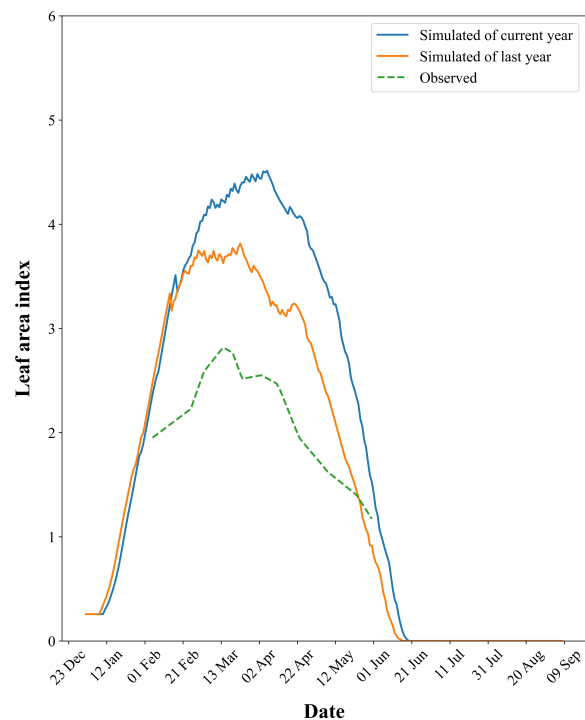
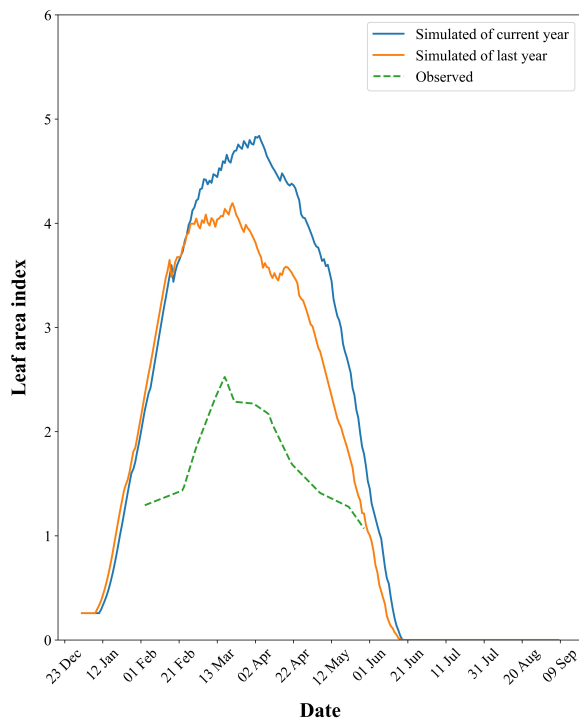
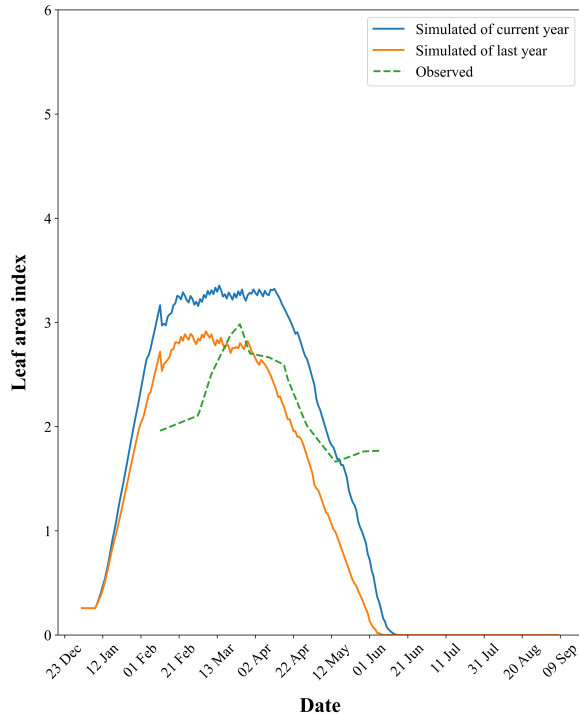


Figure 5. Temporal profiles of LAI for Canola. (a) Field 1, (b) Field 2, and (c) Field 3.

4. CONCLUSION

This study demonstrates the successful integration of Sentinel-2 multispectral imagery with an AI-driven neural network model for LAI for canola across three distinct fields, achieving high spatiotemporal resolution. The methodology effectively combines spectral reflectance data (green, red, and near-infrared bands) with solar-sensor geometry parameters to characterize canola's unique canopy structure and phenological dynamics. Validation results, including an RMSE of 208.81 and R^2 of 0.70, confirm the model's accuracy in capturing field-specific growth patterns, as evidenced by the close alignment between simulated and observed LAI values across all study sites.

The model's ability to track canola's prolonged canopy development phase, particularly the variations in peak LAI timing and magnitude among fields 1 to 3, highlights its operational value for precision agriculture. By delivering reliable, pixel-level LAI estimates, this approach enables data-driven decisions for irrigation scheduling, nutrient management, and yield optimization tailored to canola's growth stages. Furthermore, the integration of WOFOST-derived ideal LAI benchmarks provides actionable insights into field-specific constraints, bridging the gap between potential and actual crop performance.

Future research should explore the incorporation of multi-scale remote sensing data (e.g., UAV imagery for sub-field heterogeneity) and expansion to diverse agroclimatic regions to enhance model generalizability. This work underscores the transformative potential of combining satellite remote sensing with AI-driven modelling to advance sustainable canola production, offering a scalable solution for improving agricultural productivity and resource efficiency.

ACKNOWLEDGEMENTS

The authors gratefully acknowledge the support and resources provided by Basysco Remote Sensing Institute, which contributed significantly to the completion of this work.

REFERENCES

- Abdali, E., Valadan Zoej, M. J., Taheri Dehkordi, A., Ghaderpour, E., 2024. A Parallel-Cascaded Ensemble of Machine Learning Models for Crop Type Classification in Google Earth Engine Using Multi-Temporal Sentinel-1/2 and Landsat-8/9 Remote Sensing Data. *Remote Sensing*, 16(1), 127. <https://doi.org/10.3390/rs16010127>
- Alshaya, S., 2025. Precision Agriculture Based on Machine Learning and Remote Sensing Techniques. *Proceedings of the Bulgarian Academy of Sciences*. <https://doi.org/10.7546/crabs.2025.01.12>
- Csikós, N., Szabó, B., Hermann, T., Laborczi, A., Matus, J., Pásztor, L., Szatmári, G., Takács, K., Tóth, G., 2023. Cropland Productivity Evaluation: A 100 m Resolution Country Assessment Combining Earth Observation and Direct Measurements. *Remote Sensing*, 15(5), 1236. <https://doi.org/10.3390/rs15051236>
- Djamai, N., Fernandes, R., Weiss, M., McNairn, H., Goita, K., 2019. Validation of the Sentinel Simplified Level 2 Product Prototype Processor (SL2P) for mapping cropland biophysical variables using Sentinel-2/MSI and Landsat-8/OLI data. *Remote Sensing of Environment*, 225, 416–430. <https://doi.org/https://doi.org/10.1016/j.rse.2019.03.020>
- Escolà, A., Badia, N., Arnó, J., Martínez-Casasnovas, J., 2017. Using Sentinel-2 images to implement Precision Agriculture techniques in large arable fields: First results of a case study. *Advances in Animal Biosciences*, 8(2), 377–382. <https://doi.org/10.1017/S2040470017000784>
- Hassanpour, R., Majnooni-Heris, A., Fard, A., Verrelst, J., 2024. Monitoring Biophysical Variables (FVC, LAI, LCab, and CWC) and Cropland Dynamics at Field Scale Using Sentinel-2 Time Series. *Remote Sensing*, 16(13), 2284. <https://doi.org/10.3390/rs16132284>
- Hemmati, E., Sahebi, M. R., 2024. Surface soil moisture retrieval based on transfer learning using SAR data on a local scale. *International Journal of Remote Sensing*, 45(7), 2374–2406. <https://doi.org/10.1080/01431161.2024.2329529>
- Kirk, D., Cohen, J., Nguyen, V., Childs, M., Farnier, J., Davies, T., Flory, S., Rohr, J., O'Connor, M., Mordecai, E., 2025. Impacts of Weather Anomalies and Climate on Plant Disease. *Ecology Letters*, 28(1), e70062. <https://doi.org/10.1111/ele.70062>
- Li, M., Shamshiri, R., Weltzien, C., Schirrmann, M., 2022. Crop Monitoring Using Sentinel-2 and UAV Multispectral Imagery: A Comparison Case Study in Northeastern Germany. *Remote Sensing*, 14(17), 4426. <https://doi.org/10.3390/rs14174426>
- Liu, T., Duan, S., Liu, N., Wei, B., Yang, J., Chen, J., Zhang, L., 2024. Estimation of crop leaf area index based on Sentinel-2 images and PROSAIL-Transformer coupling model. *Computers and Electronics in Agriculture*, 227, 109663. <https://doi.org/10.1016/j.compag.2024.109663>
- L., P., 2024. Efficient Model on Crop Disease and Pest Detection with Deep Learning. *International Journal of Scientific Research in Engineering and Management*. <https://doi.org/10.55041/ijrem30880>
- Mostafiz, R., Noguchi, R., Ahamed, T., 2021. Agricultural Land Suitability Assessment Using Satellite Remote Sensing-Derived Soil-Vegetation Indices. *Land*, 10(2), 223. <https://doi.org/10.3390/land10020223>
- Nguyen, L., Robinson, S., Galpern, P., 2022. Medium-resolution multispectral satellite imagery in precision agriculture: mapping precision canola (*Brassica napus* L.) yield using Sentinel-2 time series. *Precision Agriculture*, 23, 1051–1071. <https://doi.org/10.1007/s11119-022-09874-7>
- Padilla, F., Farneselli, M., Gianquinto, G., Tei, F., Thompson, R., 2020. Monitoring nitrogen status of vegetable crops and soils for optimal nitrogen management. *Agricultural Water Management*, 241, 106356. <https://doi.org/10.1016/j.agwat.2020.106356>
- Pokhariyal, S., Patel, N., Govind, A., 2023. Machine Learning-Driven Remote Sensing Applications for Agriculture in India—A Systematic Review. *Agronomy*, 13(9), 2302. <https://doi.org/10.3390/agronomy13092302>
- Romero, F., Labouyrie, M., Orgiazzi, A., Ballabio, C., Panagos, P., Jones, A., Tedersoo, L., Bahram, M., Guerra, C., Eisenhauer, N., Tao, D., Delgado-Baquerizo, M., García-Palacios, P., Van Der Heijden, M., 2024. Soil health is associated with higher primary productivity across Europe. *Nature Ecology & Evolution*. <https://doi.org/10.1038/s41559-024-02511-8>
- Segarra, J., Buchaillot, M., Araus, J., Kefauver, S., 2020. Remote Sensing for Precision Agriculture: Sentinel-2 Improved Features and Applications. *Agronomy*, 10(5), 641. <https://doi.org/10.3390/agronomy10050641>
- Sishodia, R., Ray, R., Singh, S., 2020. Applications of Remote Sensing in Precision Agriculture: A Review. *Remote Sensing*, 12(19), 3136. <https://doi.org/10.3390/rs12193136>
- Srivastav, A., Dhyani, R., Ranjan, M., Madhav, S., Sillanpää, M., 2021. Climate-resilient strategies for sustainable management of water resources and agriculture. *Environmental Science and Pollution Research*, 28, 41576–41595. <https://doi.org/10.1007/s11356-021-14332-4>
- Wang, J., Wang, Y., Li, G., Qi, Z., 2024. Integration of Remote Sensing and Machine Learning for Precision Agriculture: A Comprehensive Perspective on Applications. *Agronomy*, 14(9), 1975. <https://doi.org/10.3390/agronomy14091975>
- Wang, X., Zeng, H., Yang, X., Shu, J., Wu, Q., Que, Y., Yang, X., Yi, X., Khalil, I., Zomaya, A., 2025. Remote sensing revolutionizing agriculture: Toward a new frontier. *Future Generation Computer Systems*, 166, 107691. <https://doi.org/10.1016/j.future.2024.107691>
- Weiss, M., Jacob, F., Duveiller, G., 2020. Remote sensing for agricultural applications: A meta-review. *Remote Sensing of*

Environment, 236, 111402.
<https://doi.org/10.1016/j.rse.2019.111402>

West, H., Quinn, N., Horswell, M., White, P., 2018. Assessing Vegetation Response to Soil Moisture Fluctuation under Extreme Drought Using Sentinel-2. *Water*, 10(7), 838. <https://doi.org/10.3390/w10070838>

Zhao, K., Wu, S., Liu, C., Wu, Y., Efremova, N., 2023. Precision Agriculture: Crop Mapping using Machine Learning and Sentinel-2 Satellite Imagery. *arXiv*. <https://doi.org/10.48550/arXiv.2403.09651>

Zhao, Y., Chen, H., Sun, H., Yang, F., 2024. In the Qaidam Basin, Soil Nutrients Directly or Indirectly Affect Desert Ecosystem Stability under Drought Stress through Plant Nutrients. *Plants*, 13(13), 1849. <https://doi.org/10.3390/plants13131849>